Proc. Nat. Acad. Sci. USA
Vol. 73, No. 4, pp. 1078–1082, April 1976
Biochemistry

A thermodynamic model of regulation: Modulation of redox equilibria in camphor monoxygenase

(biochemical regulation/free energy/redox potentials/cytochrome *P*-450 monoxygenase)

S. G. SLIGAR AND I. C. GUNSALUS

Department of Biochemistry, University of Illinois, Urbana, Ill. 61801

Contributed by I. C. Gunsalus, January 14, 1976

ABSTRACT **Regulation of biological phenomena occurs in all types of systems, being manifested in many different reaction types, from allosteric behavior in proteins, through modulation in energy and information transfer, to the control of growth and differentiation in cells, organelles, and organisms. In this communication, a modulation in oxidation/reduction potential via ligation of substrate and protein components in the camphor 5-*exo*-monoxygenase system is described in terms of a four-state system using as fundamental parameters the transition free energies between equilibrium states. This approach provides a concise description of the data and is useful for describing many aspects of regulatory phenomena.**

The *P*-450 camphor hydroxylase isolated from the soil bacterium *Pseudomonas putida* has provided an ideal system for the study of electron transport and mixed function oxidation reactions. This monoxygenase with the overall reaction scheme shown in Fig. 1 has been extensively reviewed (1, 2). The *P*-450 cytochrome [termed cytochrome *m* and abbreviated cyt *m*, or *m*, for monoxygenase (3)] is a 45,000 dalton heme protein which is isolated in the ferric substrate-free form (abbreviated m^o). Fig. 1 depicts the subsequent reactions: substrate (camphor) binding ($m^o + S \rightarrow m^{os}$), reduction of the heme iron to the ferrous state ($m^{os} + e^- \rightarrow m^{rs}$), binding of atmospheric dioxygen ($m^{rs} + O_2 \rightarrow m^{rs}{}_{O_2}$), and, together with the input of a second reducing equivalent, the reductive cleavage of dioxygen with one atom inserted in an oxygenation step as a hydroxyl group at the 5-*exo* position of the camphor skeleton and the second oxygen atom reduced to water. The two required reducing equivalents are supplied from NADH, through a flavoprotein reductase (abbreviated fp) and an Fe_2S_2*Cys_4 redoxin (termed putidaredoxin and abbreviated Pd; S* is labile sulfide). In this communication we present a general thermodynamic model of biochemical regulation and apply this to the modulation and control of the oxidation/reduction potentials of the redoxin and cytochrome components of the methylene hydroxylase via ligation reactions.

Interacting multiligand equilibria in proteins are presented in an elegant and transparent fashion by the free-energy description provided by Weber (4). This model of free energy changes can be extended to consider the regulation of an internal equilibrium, such as redox potential, by ligation. The modulation of a biological equilibrium reaction via the binding of a regulatory molecule is viewed thermodynamically as a four-state system, Fig. 2. In this description, the two native states A and B are in equilibrium, defined by a constant, K_N, or alternatively by a free energy, $\Delta G_N = RT \ln (K_N)$. The regulatory molecule R can bind to either the A or B form; $A + R \rightleftharpoons A{\cdot}R$, or $B + R \rightleftharpoons B{\cdot}R$. These reactions are described by dissociation constants K_A and K_B or binding free energies $\Delta G_A = RT \ln (K_A)$ and $\Delta G_B = RT \ln (K_B)$, respectively. The regulated equilibrium $A{\cdot}R \rightleftharpoons B{\cdot}R$ is described by a constant K_R or free energy $\Delta G_R = RT \ln (K_R)$. If the ligation occurs at a single locus and under conditions of unity activity coefficients, the four states shown in Fig. 2 constitute a closed cycle, with the following condition on the individual free energies:

$$\Delta G_A + \Delta G_R = \Delta G_N + \Delta G_B \qquad [1]$$

It is immediately apparent that the presentation of the regulation in terms of the relevant free energy changes offers a transparent and concise description of these phenomena. From Fig. 2 it is clear that if $\Delta G_A = \Delta G_B$ then $\Delta G_N = \Delta G_R$, that is, if there is equal affinity of R for both the A and B forms, then the constants describing the internal equilibria must necessarily be equal. For the association of R to modulate the $A \rightleftharpoons B$ equilibrium, it *must* bind tighter to either the A or B form. If R shows preferential association to A, the equilibrium is shifted toward the A form, whereas if R binds tighter to B, the resulting B·R state will be in excess over the A·R state. Thus regulation can be viewed as an asymmetric binding which then controls the internal equilibrium desired. It is important to note that in no case is it energetically possible to transform the equilibrium completely to either the A or B form. From Eq. 1 it follows that

$$-RT \ln \left[\frac{K_N}{K_R}\right] = \Delta G_B - \Delta G_A \qquad [2]$$

and hence for either K_N or K_R to approach zero an infinite change in free energy is required. However, since a difference in binding energy of only 2.7 kcal/mol is required for $K_R = 100\ K_N$, biochemical regulation can involve relatively small energy changes; often these small energy differences act in the neighborhood of unity equilibrium constants, where the regulation is most sensitive. For an equilibrium $A \rightleftharpoons B$ described by a constant $K = [A]/[B]$, the fraction of the population in the B form, f_B, is

$$f_B = \frac{1}{1 + K} = \frac{1}{1 + e^{+\Delta G/RT}} \qquad [3]$$

The rate of change of f_B with change in free energy ΔG

$$\frac{df_B}{d\Delta G} = \frac{-1}{RT}\left[\frac{e^{+\Delta G/RT}}{[1 + e^{+\Delta G/RT}]^2}\right] \qquad [4]$$

Abbreviations: Pd, putidaredoxin; cytochrome *m* or cyt *m*, cytochrome *P*-450 camphor monoxygenase. Abbreviations as to redox state and substrate association are indicated as superscripts: m^o, oxidized (ferric) protein; m^r, reduced (ferrous) state; and m^s, substrate bound. Heme ligands are indicated by subscripts, i.e., $m^{rs}{}_{O_2}$, oxygenated ferrous substrate-bound cytochrome.

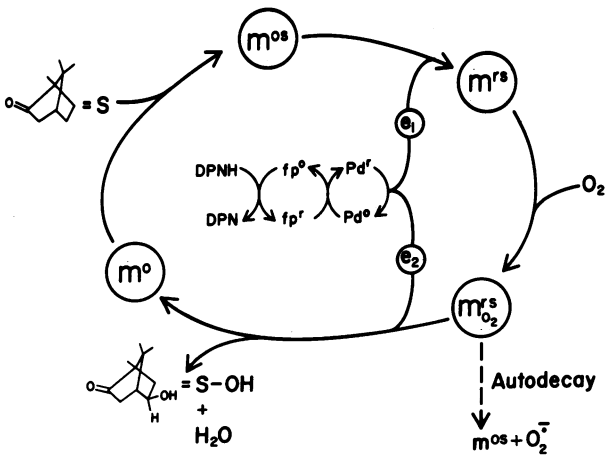

FIG. 1. Camphor 5-*exo* hydroxylase reaction cycle. Cytochrome *m* is labeled according to redox and ligand states as described in the *text*. The two electrons (e_1 and e_2) required for dioxygen cleavage are supplied from DPNH via a flavoprotein reductase (fp) and putidaredoxin (Pd).

is maximum at $\Delta G = 0$. Hence, modulation near zero free energy change results in the greatest sensitivity in regulation.

We now proceed to illustrate the utility of this model of regulation by considering the modulation in the oxidation/reduction potential of the protein components of the camphor monoxygenase system via asymmetric ligation reactions.

MATERIALS AND METHODS

Putidaredoxin and cytochrome *m* were purified from *Pseudomonas putida* strain PpG786, grown on camphor as a sole source of carbon and energy as previously reported (5, 6). Both redoxin and cytochrome were obtained in pure, homogeneous form, with recrystallization of cyt *m* as a final purification step (7). Physical properties of Pd and cyt *m*, including extinction coefficients, used in this investigation are summarized in ref. 2. Preparation of fluorescein-isothiocyanate-labeled cyt *m* was previously described (3). Redox potentials were determined photochemically (3). The recrystallized dye Brilliant Alizarin Blue (Hartman-Leddon Co., Philadelphia) with a standard $E_o' = -173$ mV (8) was mixed with an equal concentration of Pd^o and m^{os} in 50 mM potassium phosphate buffer, pH 7.0, containing 10 mM EDTA and 500 μM camphor, in high enough concentration to saturate the Pd–cyt *m* association. Electrons were added to the equilibrium by irradiating the reaction mixture with white light from a 300 W projection bulb (9), and the concentration of Pd reduced was determined by the optical absorption at 404 nm (an isosbestic point for $m^{os} \rightleftharpoons m^{rs}$), while the fraction of cyt *m* reduced was observed by monitoring at 391 nm after correction for the small absorbance changes of redoxin at this wavelength. The concentration of reduced dye was determined by the absorption at 520 nm after deconvoluting the contributions due to protein absorbances. All data were analyzed according to the Nernst equation:

$$E_D = E_{oD}' + \frac{RT}{nF} \ln\left[\frac{f_D^{\,o}}{f_D^{\,r}}\right] = E_P = E_{oP}' + \frac{RT}{nF} \ln\left[\frac{f_P^{\,o}}{f_P^{\,r}}\right] \quad [5]$$

where $E_D = E_P$ are the total system potentials for dye and protein, respectively, and fs are the redox fractions.

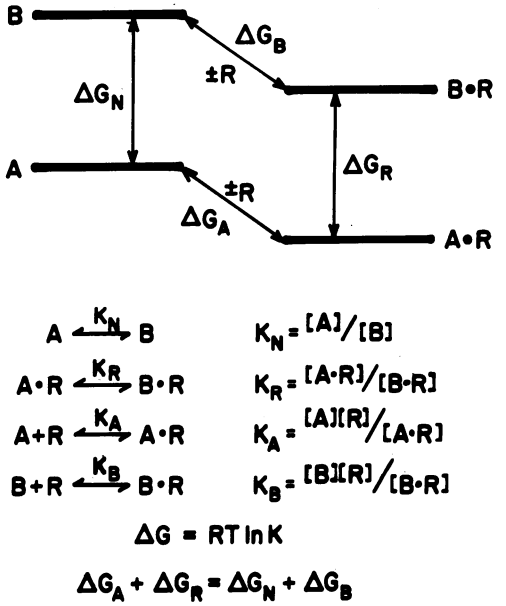

FIG. 2. Thermodynamic model of regulation. The modulation of the A ⇋ B equilibrium constant via asymmetric association of the regulatory molecule R is illustrated. Both ligation and internal equilibria are described by free energies ΔG. ΔG_N and ΔG_R represent the native and regulated processes, while ΔG_A and ΔG_B represent the free energies for binding R to the A and B forms. Conservation of energy requires that $\Delta G_A + \Delta G_R = \Delta G_N + \Delta G_B$ which is equivalently expressed in terms of equilibrium constants: $K_A K_R = K_N K_B$.

Data acquisition and processing were accomplished on-line with a Wang System 600 digital computer. In order to improve the signal-to-noise ratio, 100 absorbance readings at each wavelength were averaged at 0.5 second intervals. After computer deconvolution of the overlapping spectra and subsequent analysis, results were presented in graphic form on a Wang model 600 plotting output writer.

All chemicals used were analytical grade as supplied by Aldrich Chemical Co.

RESULTS

Modulation of cytochrome redox potentials by asymmetric camphor ligation

The heme iron of cytochrome *m* contains a one-electron ferric/ferrous couple. We now consider the modulation in this equilibrium via the association of the substrate camphor (10). Fig. 3 depicts the four states of this couple according to the model described in the introduction. ΔG_1 represents the free energy of the redox equilibrium for the substrate-free cytochrome ($m^o \rightleftharpoons m^r$), and ΔG_2 that of the substrate-bound cytochrome ($m^{os} \rightleftharpoons m^{rs}$). These free energies are related to the more commonly used redox potentials via the relation $\Delta G = -F\Delta E_o'$. ΔG_3 and ΔG_4 represent the substrate binding free energies for the oxidized ($m^o + S \rightleftharpoons m^{os}$) and reduced ($m^r + S \rightleftharpoons m^{rs}$) cytochrome, related to the measured dissociation constants, K_D, via the relation $\Delta G = RT \ln (K_D)$. Again, it is clear from the graphic model (Fig. 3) that in order for the redox equilibria of cytochrome *m* to be modulated by substrate, there must be an asymmetric association of camphor to the oxidized and reduced forms. The converse is also valid in that if one observes an asymmetry in binding to oxidized and reduced forms, then the association must necessarily change the redox potential. Due to the microreversibility between redox and substrate equilib-

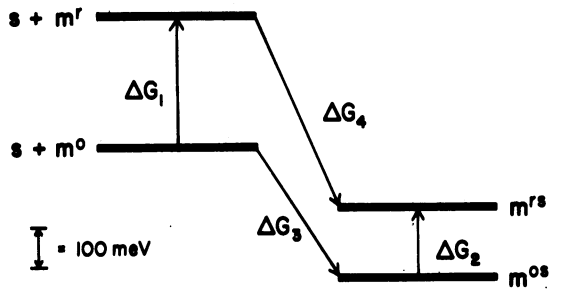

FIG. 3. Substrate modulation of cytochrome m redox potential. The asymmetric association of the substrate camphor to oxidized ($m^o + S \rightleftharpoons m^{os}$) and reduced ($m^r + S \rightleftharpoons m^{rs}$) forms of the cytochrome is reflected by a corresponding shift in the equilibrium redox potentials. In this scale drawing ΔG_1 and ΔG_2 represent the redox potentials of substrate-free and substrate-bound forms, respectively. ΔG_3 and ΔG_4 are the camphor binding energies; the former to m^o, the latter to m^r. See Table 1 for numerical values.

ria, the free energy changes around the diagram must sum to zero, $\Delta G_1 + \Delta G_4 = \Delta G_2 + \Delta G_3$. The redox potentials of $m^{os} \rightleftharpoons m^{rs}$ and $m^o \rightleftharpoons m^r$, together with the substrate dissociation constants for binding to the oxidized and reduced forms, are summarized in Table 1 and Fig. 3. When values of ΔG_1, ΔG_2, and ΔG_3 are used to calculate ΔG_4, representing the association of camphor to ferrous cytochrome m, excellent agreement with the measured values is observed, illustrating the predictive value of the energetic approach.

This analysis, however, does not completely describe the response of the cytochrome m ferric/ferrous reduction to other external ligation and internal equilibria. Potassium and proton binding are known to couple with the reactions described and the internal spin state equilibria further divide the energy levels. These reactions, together with an extension of the thermodynamic regulatory model to include the enthalpy and entropy state functions, are described in ref. 11. However, in considering only these four states of the total interacting equilibria, the presentation of the data in terms of a free energy diagram offers a clear picture of ligation-induced regulation. This diagrammatic method becomes increasingly more valuable with more than one interacting species and is almost mandatory when one considers ligation of components containing more than one redox center, as is the case for the association between putidaredoxin and cytochrome m.

Putidaredoxin-cytochrome m binding and redox transfer

Referring to Fig. 1, the first step in the formation of the oxygenated intermediate $m^{rs}{}_{O_2}$ is the Pd-mediated ferric/ferrous reduction of the cyt m heme iron, given by the overall reaction $m^{os} + Pd^r \rightarrow m^{rs} + Pd^o$. A natural question is whether this electron transfer reaction proceeds through the

Table 1. Substrate modulation of cytochrome m redox potential

Reaction	ΔG (meV)	K_D (M)	Ref.
1. $m^o \leftrightharpoons m^r$	+340		10
2. $m^{os} \leftrightharpoons m^{rs}$	+170		10, 12
3. $m^o + S \leftrightharpoons m^{os}$	−325	3.6×10^{-6}	2
4. $m^r + S \leftrightharpoons m^{rs}$			
Calculated	−495	5.1×10^{-9}	
Measured	−498	4.5×10^{-9}	16

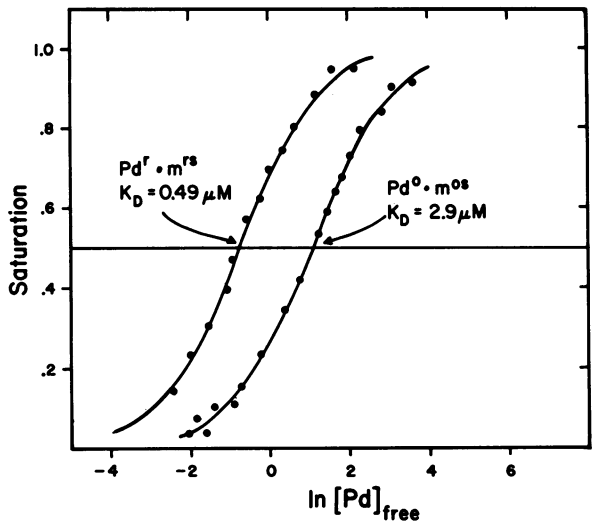

FIG. 4. Asymmetric binding of putidaredoxin to cytochrome m in the oxidized and reduced states. Conditions are as described in the *text*.

formation of a long-lived Pd-cyt m complex. The binding of redoxin to cytochrome can be followed by the quenching of the fluorescence of a fluorescein isothiocyanate group covalently attached to an external sulfhydryl on the cytochrome surface (3). Fig. 4 shows the standard analysis of the binding experiment, plotting the site saturation versus the natural logarithm of free Pd concentration. The binding of Pd^o to m^{os} exhibits a one-to-one stoichiometry at this locus, with a dissociation constant of 2.9 μM at 283 K (3), corresponding to a binding free energy of −307 meV (−7.06 kcal/mol, 29.5 kJ/mol). When the titration is carried out with the reduced proteins under the same anaerobic conditions except for the addition of a 2-fold excess of sodium dithionite, a shift in the dissociation constant to 0.49 μM is observed, corresponding to a binding free energy of −350 meV (−8.05 kcal/mol). This asymmetry in the association of Pd to cytochrome m depending on the redox state of the proteins leads to a corresponding shift in the equilibrium redox potential of Pd or cytochrome m. These potentials are measured as described in *Materials and Methods*. Fig. 5 shows a standard analysis of the Nernst equation, where the natural log of the fractional ratio of protein reduced/oxidized is plotted as a function of the total system potential. The natural log-zero intercept corresponding to equal concentrations of oxidized and reduced protein defines the equilibrium potential. The E_o' for Pd-$m^{os} \rightleftharpoons$ Pd-m^{rs} is measured to be −173 mV, in excellent agreement with values published for the free cytochrome ($m^{os} \rightleftharpoons m^{rs}$), −170 mV (10). The redoxin equilibrium, however, shows a substantial shift, from −239 mV measured for free Pd ($Pd^o \rightleftharpoons Pd^r$) (12), to −196 mV for Pd bound to cytochrome m. These values, when converted to free energies, can be coupled with the binding free energies to construct an energy diagram for the ligation and redox equilibrium, Fig. 6. Since we have in this case a total of three equilibria, two redox and one ligation, there are $2^3 = 8$ states of the system. The left side of Fig. 6 represents the redox potential energies of the protein components free in solution, the right side the corresponding potentials of the redox couples in the dienzyme complex. The two sets of states are connected via the binding free energies of the various components. The measured and calculated free energy changes, are summarized in Table 2. Although ΔG_9 and ΔG_{10} cannot be measured independently due to the rapid

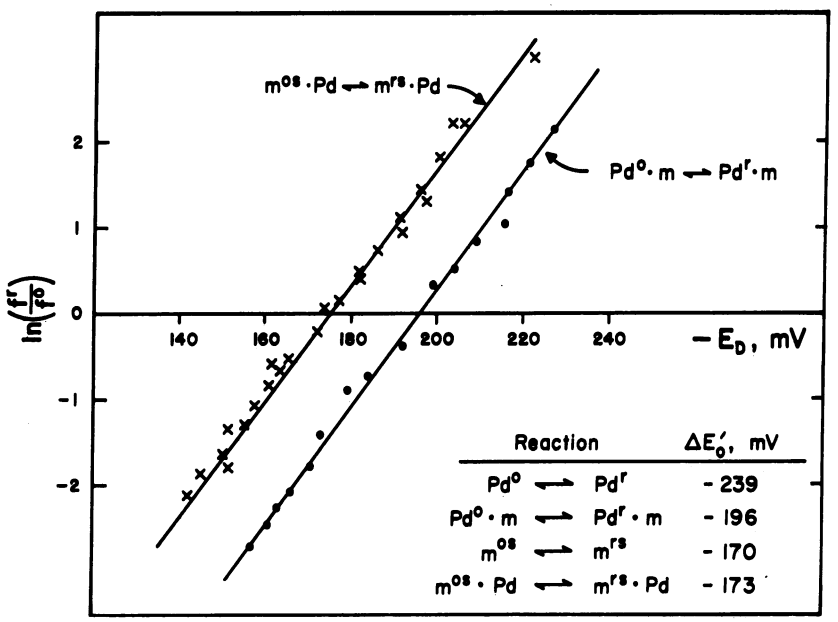

FIG. 5. Oxidation/reduction potentials of putidaredoxin and cytochrome *m*, free, and bound as a dienzyme complex. The natural log of the fraction of protein reduced over the fraction oxidized is plotted as a function of the total system potential, E_D. A substantial shift in the potential of putidaredoxin is observed on binding to the cytochrome.

electron transfer reaction, it is evident from the conditions of energy conservation under equilibrium conditions and the linearity in potential titrations that the asymmetry in the association of protein components at this site is due to the redox state of putidaredoxin, and the ligation reaction is unaffected by the redox state of cytochrome *m*. With the values summarized in Fig. 6 and Table 2, one can calculate ΔG_6, the actual potential through which the reducing equivalent is transferred from the redoxin to the cytochrome in the dienzyme complex. This value is 23 meV as opposed to what one would calculate using the free potentials $|\Delta G_2 - \Delta G_1| = 69$ meV. Energetically speaking, a portion of the free energy available in the Pd/*m* redox couple is expended in order to provide a more selective association of Pd^r at this locus. As shown in Fig. 7, this corresponds to an equilibrium constant k_2/k_{-2} of 2.6, and hence the equilibrium is shifted much more toward equipotential transfer. (A free energy change of 70 meV would correspond to an equilibrium constant of 18.) The observed redox potential changes fitted together with the asymmetry in association of oxidized and reduced proteins at a specific site strongly suggest that the electron transfer proceeds through the observed dienzyme complex intermediate. Applying the converse argument, if a change in redox potential of a species is observed, directly related to and depending upon whether this species is free or bound to another molecule, then there must necessarily be an asymmetry in the association constants of these molecules depending upon the redox state of the components. Thus, it having been observed that when Pd and cyt *m* are mixed with reducing equivalents, the equilibrium concentration of reduced cytochrome is considerably different than that calculated from the free potentials in the overall reaction $Pd^r + m^{os} \rightleftharpoons Pd^o + m^{rs}$, the simplest model to account for this change is the introduction of asymmetric binding steps as shown in Fig. 7. This does not change the overall energy difference in the reaction $Pd^r + m^{os} \rightleftharpoons Pd^o + m^{rs}$, but shifts

Table 2. Pd and cyt *m* ligation and redox equilibria

Parameter	ΔG (meV)	Ref.
ΔG_1	170	10
ΔG_2	239	10, 12
ΔG_4, ΔG_7	173	This work
ΔG_5	196	This work
ΔG_8	−307	This work
ΔG_{11}	−350	This work
ΔG_6	20*	This work
	23†	This work

* $\Delta G_6 = \Delta G_1 + \Delta G_2 + \Delta G_{11} - \Delta G_8 - \Delta G_4 - \Delta G_7$.
† $\Delta G_6 = \Delta G_5 - \Delta G_4$.

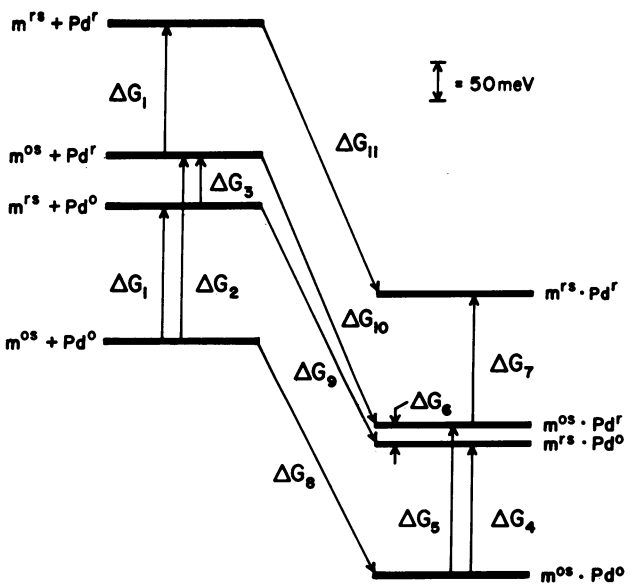

FIG. 6. Energy states of Pd and cytochrome *m*. The redox states of the isolated protein components are shown to scale on the left side, with those of the dienzyme complex on the right. The two manifolds are connected by the binding free energies of the components. Numerical values are summarized in Table 2.

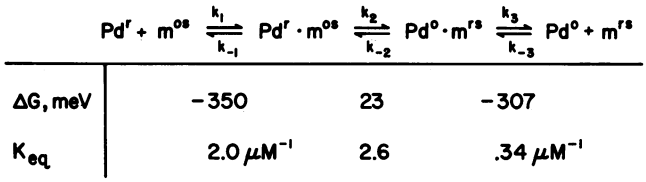

FIG. 7. Summary of the Pd/cyt *m* coupled redox and ligand equilibria. The electron transfer between redoxin and cytochrome proceeds through a specific complex between the protein components.

the measured intermediate equilibrium $Pd^{r} \cdot m^{os} \rightleftharpoons Pd^{o} \cdot m^{rs}$. Elegant kinetic measurements of the redoxin to cytochrome electron transfer by T. Pederson at the University of Illinois using flash photolytic and stopped flow techniques have unambiguously shown that indeed the reduction of cyt *m* by Pd proceeds through a redoxin–cytochrome complex (13). The kinetic parameters obtained are in excellent agreement with the constants derived in the equilibrium studies reported in this communication.

The shift in Pd potential on binding to cytochrome *m* may possibly indicate that the iron-sulfur active site is on the protein surface. It is known that the polarity of the local environment can affect the redox potentials of iron centers (14). If association between redoxin and cytochrome is through mutual hydrophobic interaction as tentatively proposed (3), such association near the iron-sulfur center could induce the observed potential shift.

SUMMARY

We have presented a simple description for the regulation and control of biochemical equilibria. Illustrative examples of the utility of this method are taken from studies on the oxidation/reduction potentials of protein components of the camphor monoxygenase system from *Pseudomonas putida*. Coupled equilibria are best presented in terms of the free energy coupling model described here, a direct outgrowth of the elegant formalism developed by Gregorio Weber at the University of Illinois (4, 15). The complete documentation of all interacting reactions in the camphor monoxygenase is far from complete. The large number of reactions constitutes an *n*-dimensional space of equilibria, and future descriptions of multicomponent reactions will treat the total system energy as a functional of these equilibria, with graphic presentation of two and three component subspaces describing modulated reactions.

The expert and untiring assistance of Ms. M. J. Namtvedt is gratefully acknowledged. The authors wish to thank Gregorio Weber, Peter Debrunner, John Lipscomb, and Thomas Pederson for many valuable discussions, and Ms. Kathryn Skelton for editorial assistance. This work was supported by a grant from the National Institutes of Health, PHS GM 21161.

1. Gunsalus, I. C., Pederson, T. C. & Sligar, S. G. (1975) *Annu. Rev. Biochem.* **44**, 377–407.
2. Gunsalus, I. C., Meeks, J. R., Lipscomb, J. D., Debrunner, P. & Münck, E. (1974) in *Molecular Mechanisms of Oxygen Activation*, ed. Hayaishi, O. (Academic Press, New York), pp. 559–613.
3. Sligar, S., Debrunner, P., Lipscomb, J., Namtvedt, M. J. & Gunsalus, I. C. (1974) *Proc. Nat. Acad. Sci. USA* **71**, 3906–3910.
4. Weber, G. (1972) *Biochemistry* **11**, 864–878.
5. Yu, C.-A. & Gunsalus, I. C. (1974) *J. Biol. Chem.* **249**, 94–101.
6. Garg, G. K., Toscano, W. A. & Gunsalus, I. C. (1976) *J. Biol. Chem.*, in press.
7. Yu, C.-A. & Gunsalus, I. C. (1970) *Biochem. Biophys. Res. Commun.* **40**, 1431–1436.
8. Sober, J. A., ed. (1970) *Handbook of Biochemistry* (Chemical Rubber Company, Cleveland, Ohio).
9. Greenbaum, E., Austin, R. H., Frauenfelder, H. & Gunsalus, I. C. (1972) *Proc. Nat. Acad. Sci. USA* **69**, 1273–1276.
10. Lipscomb, J. D. (1974) Ph.D. Dissertation, University of Illinois, Urbana.
11. Sligar, S. G. (1976) *Biochemistry*, in press.
12. Wilson, G. S., Tsibris, J. C. M. & Gunsalus, I. C. (1973) *J. Biol. Chem.* **248**, 6059–6061.
13. Pederson, T. C. & Gunsalus, I. C. (1976) *Biochim. Biophys. Acta*, in press.
14. Que, L. Jr, Anglin, J. R., Bobrik, M. A., Davison, A. & Holm, R. H. (1974) *J. Am. Chem. Soc.* **96**, 6042.
15. Weber, G. (1975) *Adv. Protein Chem.* **29**, 1–85.
16. Griffing, B. W. & Peterson, J. A. (1972) *Biochemistry* **11**, 4740–4746.